Supplementary Materials

Machine learning enhanced characterization and optimization of photonic cured $MAPbI_3$ for efficient perovskite solar cells

Cody R. Allen[1], Bishal Bhandari[1], Weijie Xu[2], Mark Lee[1], Julia W. P. Hsu[2,*]

[1]Department of Physics, The University of Texas at Dallas, Richardson, TX 75080, USA.
[2]Department of Material Science and Engineering, The University of Texas at Dallas, Richardson, TX 75080, USA.

***Correspondence to:** Dr. Julia W. P. Hsu, Department of Material Science and Engineering, The University of Texas at Dallas, 800 W Campbell Road, Richardson, TX 75080, USA. E-mail: jwhsu@utdallas.edu

Supplementary Table 1: A table containing all the photonic curing conditions including those determined by LHS (PC 1-19) and GPR (PC 20-31). Each condition has 4 uniquely determined input parameters with the radiant energy being set via adjustments to the PC voltage. The three conditions displayed in **Figure 1** are highlighted in their respective color.

PC Condition	No of µPulse (#)	Duty Cycles (%)	PC voltage (V)	PC length (ms)	Radiant Energy (J/cm²)	Procrustes Distance	Procrustes Distance w/o Scaling & Rotation	Fréchet Distance	Root Mean Square
00	12	30	318	15	3.1	1.37E-07	3.75E-07	1.88E-01	2.55E+00
01	20	60	394	45	10.2	9.39E-09	2.74E-08	4.58E-02	6.16E-01
02	27	50	432	35	12	8.57E-09	2.98E-08	5.80E-02	5.97E-01
03	5	40	356	25	6.8	5.68E-09	9.62E-09	2.84E-02	3.49E-01
04	17	45	444	30.6	12.2	8.40E-09	2.85E-08	6.35E-02	1.04E+00
05	30	40	399	48.2	10.1	5.95E-09	1.71E-08	2.18E-02	1.56E-01
06	25	60	437	10.5	9.2	7.25E-09	1.87E-08	7.22E-02	1.10E+00
07	2	35	450	47.5	13.2	5.76E-07	9.98E-06	7.81E-01	8.35E+00
08	25	50	393	27.3	9.2	2.41E-09	1.25E-08	3.80E-02	3.16E-01
09	30	45	440	25.8	11.4	2.70E-09	2.90E-09	1.83E02	2.32E-01
10	16	50	383	21.9	8.3	2.92E-09	9.75E-09	4.09E-02	4.47E-01
11	30	50	362	36.1	8	8.25E-09	5.24E-08	5.44E-02	5.58E-01
12	27	50	392	39.1	9.7	2.39E-09	5.24E-09	3.57E-02	3.52E-01
13	20	45	368	34.9	8.1	5.41E-09	4.24E-08	5.10E-02	4.32E-01
14	23	50	425	32.7	11.6	1.15E-08	2.97E-08	3.13E-02	3.13E-01
15	30	55	416	39.7	11.3	9.76E-09	2.12E-08	2.23E-02	2.06E-01
16	25	50	334	33.1	6.5	8.26E-08	1.02E-07	7.37E-02	4.36E-01

17	16	55	343	26.1	6.8	1.16E-08	1.18E-08	4.71E-02	6.39E-01
18	30	40	366	36.4	7.6	3.73E-08	1.50E-07	7.44E-02	8.76E-01
19	20	45	384	27	8.2	6.09E-09	6.53E-09	3.27E-02	3.21E-01
20	13	45	370	25	7.5	1.75E-08	4.80E-08	9.36E-02	1.31E+00
21	30	40	415	47	10.4	9.38E-09	9.46E-09	4.02E-02	7.50E-01
22	26	45	428	27	10.6	3.82E-09	9.13E-09	2.35E-02	2.57E-01
23	20	50	395	25	8.9	5.88E-09	1.77E-08	4.55E-02	3.95E-01
24	27	50	401	43	10.2	1.03E-09	8.63E-09	2.83E-02	2.60E-01
25	27	45	442	28	11.5	9.21E-10	9.29E-10	1.32E-02	1.93E-01
26	30	40	392	50	9.5	2.91E-09	3.31E-09	2.85E-02	3.01E-01
27	2	40	349	25	6.5	2.53E-08	2.09E-07	1.02E-01	1.15E+00
28	25	45	412	32	10	1.71E-08	1.60E-07	8.28E-02	8.65E-01
29	26	55	410	41	10.7	7.33E-09	5.48E-08	5.52E-02	5.48E-01
30	28	50	432	27	11.2	4.36E-09	4.68E-08	4.11E-02	2.66E-01

Supplementary Table 2: The thermal and optical properties for the simulated materials used in SimPulse® temperature simulations.

Material	**Thickness (mm)**	**Density ($g \cdot cm^{-3}$)**	**Thermal Conductivity ($W \cdot m^{-1} \cdot K^{-1}$)**	**Specific Heat ($J \cdot Kg^{-1} \cdot K^{-1}$)**	**Attenuation (cm^{-1})**
$MAPbI_3$	0.270 (measured)	4.161[1]	0.332[1]	4033[1]	45000 (measured)
ITO*	0.155	6.8	11	357	2
Glass (soda-lime)*	1100	2.52	1.1	800	0.33

* Values taken from SimPulse® simulation database

Gaussian Process Regression/Bayesian Optimization Specifics:

All four of the distance metrics were scaled and inverted. Procrustes distance, modified Procrustes distance, and Fréchet distance were scaled as:

$$scaled\ distance = \left|\log \frac{d_i}{\max(d_i)}\right|.$$

where d_i represents each distance represents the vector of all distances $\boldsymbol{d}$ and is divided by the max value of the vector. Due to being reasonably small numbers, RMS distances were simply calculated as the inverse of RMS values.

The models were built in MATLAB version 2023a using the built-in function 'fitrgp' with the input arguments:

KernelFunction: ardmatern52
ConstantSigma: true
FitMethod: none
Sigma was uniquely defined for each distance metric as (0.846, 0.869, 0.309, 1.10) in the same order as the metrics appear in the text.

Hyperparameters: Characteristic lengths were calculated by plotting each input variable against each scaled output metric. A spline was run through the data space and the average wavelength for each input variable was calculated. Scale factors were calculated as the largest – smallest scaled output metric.

Supplementary Table 3: The characteristic length scale and scale factor hyperparameters for each feature and each metric.

Model Metric	Characteristic Length Scales				Scale Factor
	Pulse Length	number of mpulses	Duty Cycle	Radiant Energy	
Procrustes	0.117	0.384	0.329	0.107	3.16
Modified Procrustes	0.090	0.378	0.379	0.097	4.07
Fréchet	0.088	0.284	0.154	0.087	1.88
RMSD	0.117	0.260	0.400	0.075	2.78

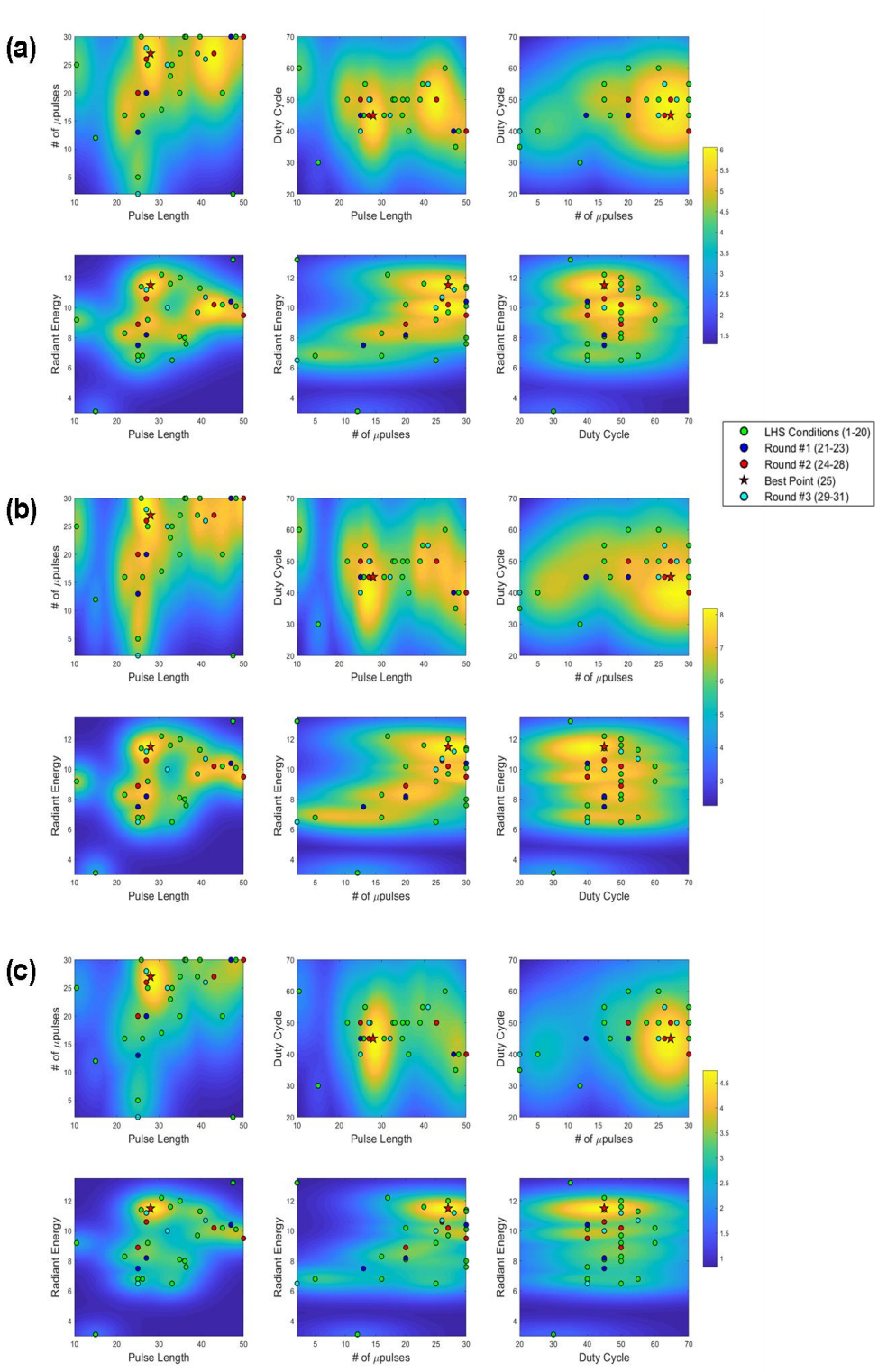

Supplementary Figure 1: Heat map plots for (a) Procrustes distance, (b) modified Procrustes distance, and (c) RMS distance

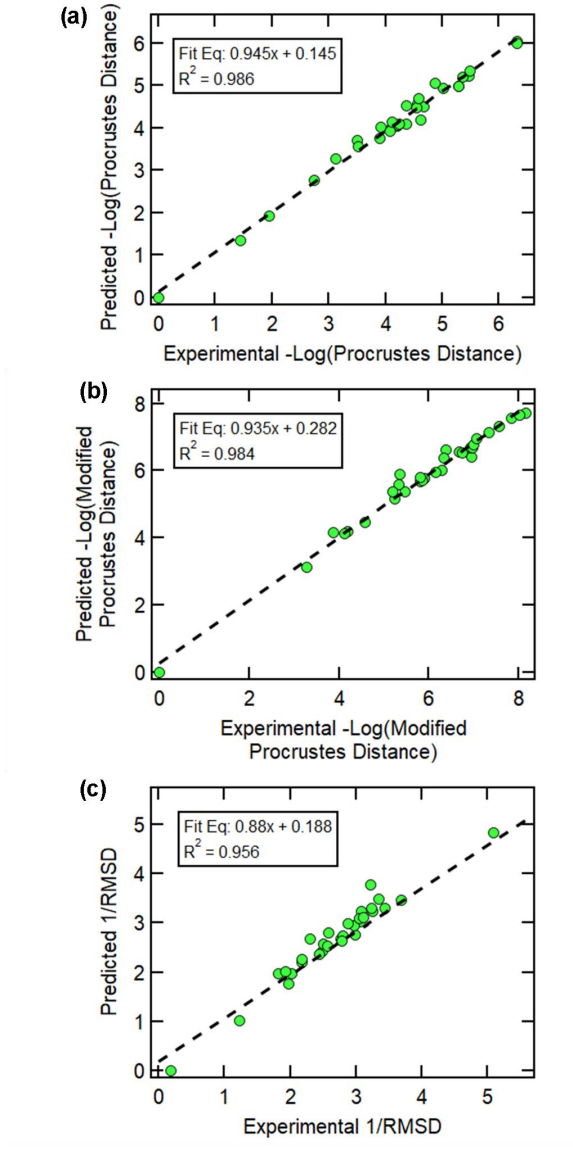

Supplementary Figure 2: Parity plots for (a) Procrustes distance, (b) modified Procrustes distance, and (c) RMS distance

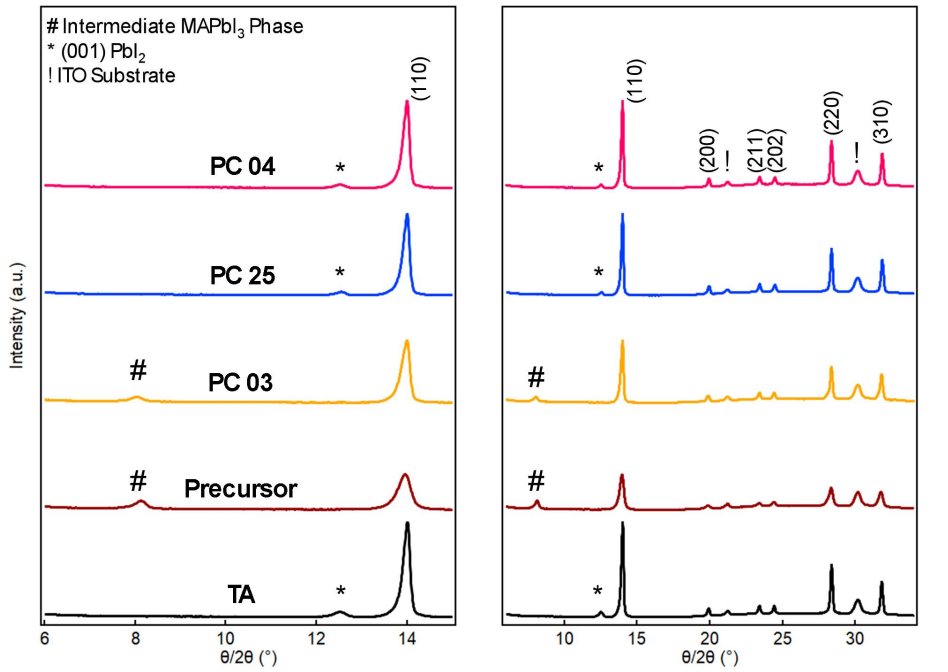

Supplementary Figure 3: X-ray diffraction (XRD) patterns for all the $MAPbI_3$ annealing conditions and precursor.

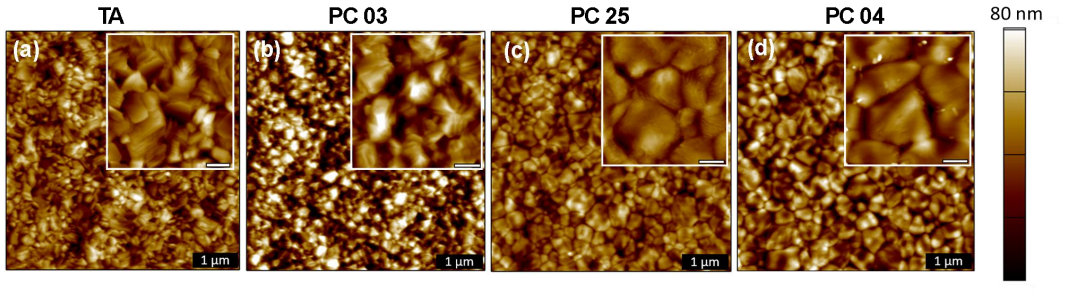

Supplementary Figure 4: Atomic force microscopy (AFM) images for the four $MAPbI_3$ annealing conditions presented in this study. Each sub-figure includes a 5 x 5 $(\mu m)^2$ overview, and an inlaid 2 x 2 $(\mu m)^2$ detailed image (scale bar = 0.5 µm). The $MAPbI_3$ annealing conditions are as follows: (a) thermal anneal, (b) PC 03 (6.8 J/cm^2), (c) PC 25 (11.5 J/cm^2), and (d) PC 04 (12.2 J/cm^2).

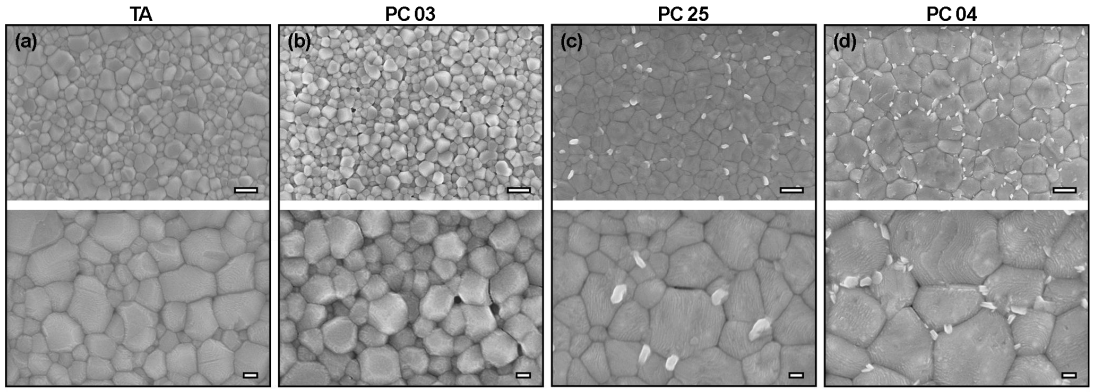

Supplementary Figure 5: Scanning electron microscopy (SEM) image for the four $MAPbI_3$ annealing conditions highlighted in the main text. Each sub-figure includes a 25,000x magnification image (scale bar = 400 μm) and a 65,000x zoom-in view (scale bar = 100 μm). The order of the $MAPbI_3$ annealing conditions is as follows: (a) thermal anneal, (b) PC 03 (6.8 J/cm^2), (c) PC 25 (11.5 J/cm^2), and (d) PC 04 (12.2 J/cm^2).

Supplementary Table 4: A statistical comparison of the accuracy of the AI segmentation model as compared to the typical ASTM E112-13 line intercept method.

	ASTM E112-13 (nm)	**AI Segmentation (nm)**
TA	161 ± 8	162 ± 62
PC 03	134 ± 7	165 ± 55
PC 25	231 ± 33	246 ± 82
PC 04	348 ± 29	312 ± 135

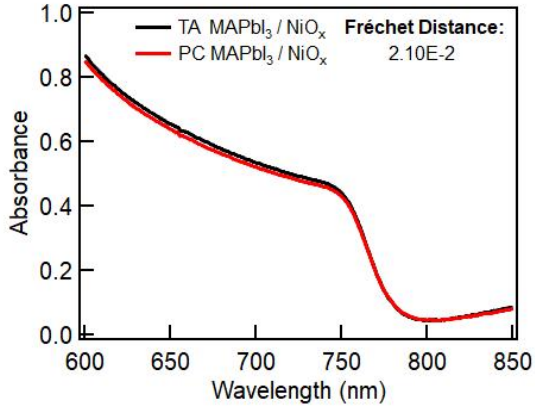

Supplementary Figure 6: UV-vis absorbance curves for devices with TA/PC $MAPbI_3$ and NiO_x as well as the associated Fréchet distances when comparing the TA/PC devices.

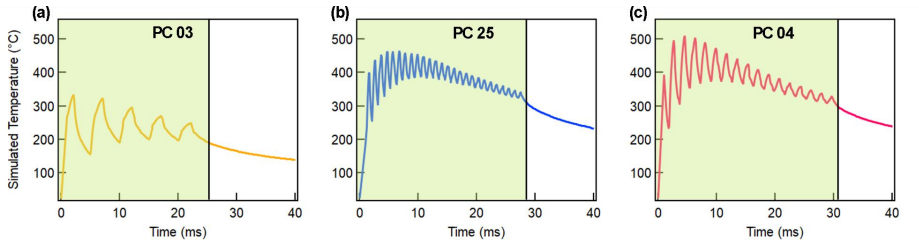

Supplementary Figure 7: Simpulse® simulations of temperature at the $MAPbI_3/NiO_x$ interface vs time for the PC 03, PC 25, and PC 04 conditions. The light-green region indicates the length of time the light is one for each condition.

Supplementary Table 5: This table shows the average *J-V* parameters for the different PSC device structures presented in this study. In this table, SAM (Self Assembled Monolayer) is used in place of MeO-2PACz.

Annealing Technique	HTL	V_{oc} (V)	J_{sc} (mA/cm^2)	FF	PCE (%)	Champion PCE (%)
TA	NiO_x	0.944 ± 0.015	17.2 ± 0.6	0.634 ± 0.071	10.3 ± 1.0	11.7
PC	NiO_x	0.773 ± 0.022	2.57 ± 1.70	0.608 ± 0.038	1.19 ± 0.75	2.42
PC	NiO_x + PbI_2	0.830 ± 0.030	9.84 ± 0.76	0.666 ± 0.045	5.43 ± 0.43	6.08
PC	NiO_x + SAM	0.953 ± 0.013	16.5 ± 0.4	0.675 ± 0.040	10.6 ± 0.6	11.8

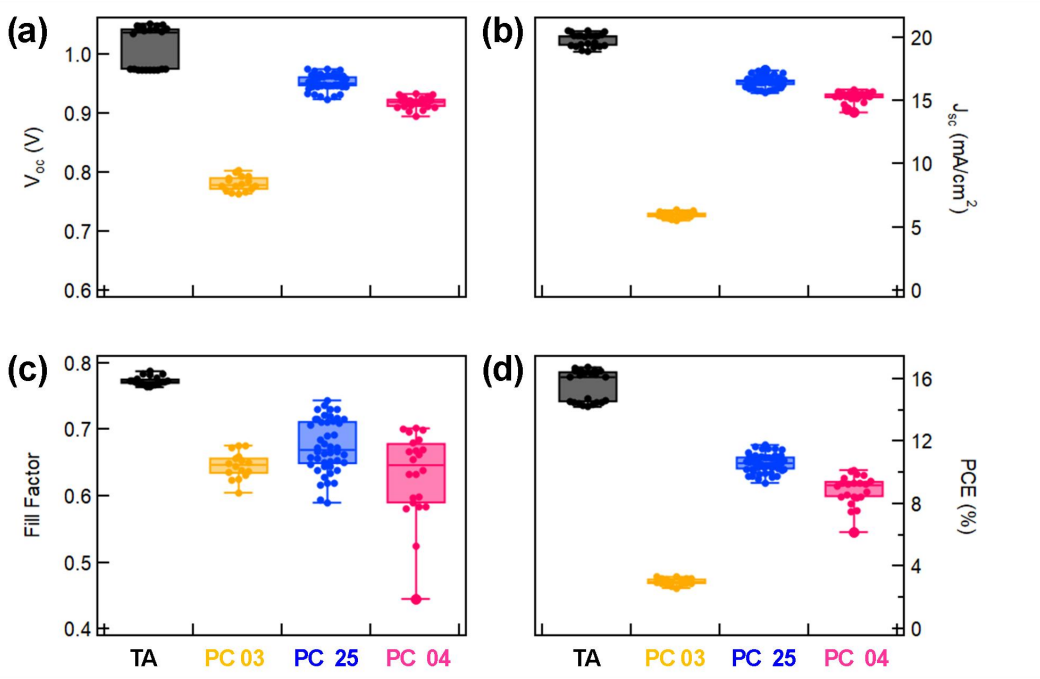

Supplementary Figure 8: Box plots for the statistical analysis of *J-V* characteristics for all TA/PC PSC devices produced with different $MAPbI_3$ annealing conditions. All PSCs contain NiO_x as the base-HLT and a 0.5 mg/ml MeO-2PACz buffer layer.

REFERENCES

1. Xu W, Daunis TB, Piper RT, Hsu JWP. Effects of Photonic Curing Processing Conditions on MAPbI $_3$ Film Properties and Solar Cell Performance. *ACS Appl Energy Mater*. 2020;3(9):8636-8645. doi:10.1021/acsaem.0c01243